# APPLICATION OF A DIAGNOSTIC NUMERICAL MODEL TO THE TROPICAL ATMOSPHERE [1]

DAVID P. BAUMHEFNER [2]

National Center for Atmospheric Research, Boulder, Colo.

## ABSTRACT

A diagnostic, nonlinear balanced model is applied in order to describe numerically the three dimensional structure of the tropical atmosphere. Several comparisons and experiments are made to gain insight into the physical processes and reliability of the model. These include different types of stream functions and temperature analyses, and the addition of surface friction and latent heat. A comparison between the kinematic vertical motion and the final numerical result is performed.

Obtained by using the complete form of the balance model, the derived vertical motion for August 12–14, 1961, in the Caribbean is presented in the form of cross sections. The vertical velocity fields, which are displayed in partitioned form, are compared with the analyzed moisture distribution. The validity of the computed vertical motion is discussed along with its possible influence on the tropical weather.

## 1. INTRODUCTION

One of the basic problems remaining in the field of tropical meteorology is the accurate description of the three dimensional velocity structure of synoptic-scale tropical disturbances. This description should include an adequate representation of the nondivergent part of the wind, commonly known as the stream function, and a calculation revealing the vertical component of velocity, which is related to the divergent part of the wind. Armed with information of this nature, the dynamics and energetics of the tropical weather systems can be investigated. The key to problems concerned with hurricane development and prediction may be found by incorporating a reliable initial state velocity structure into a prognostic model.

The early methods of obtaining a picture of the three dimensional velocity pattern were mostly qualitative in nature. The best examples of this type of research were performed by Riehl [15] and Palmer [12]. Their approach was to propose a dynamic model for some typical tropical system and imply the wind structure and vertical motion from the model. As the time and space variation of vertical wind soundings increased in number, it became feasible to calculate, in a quantitative fashion, the parameters necessary to describe the velocity field. However, a multitude of problems arose when the older schemes for computing the vertical motion, such as the adiabatic or kinematic methods, were used [13]. The most serious drawback was the extreme sensitivity to small-scale changes in the data analysis.

Because of the widespread success of the numerical process in the midlatitudes [18, 11, 7], it is proposed that a numerical model be applied to the Tropics. According to scale analysis [1], the balanced formulation of the equations of motion is valid in the Tropics if the Rossby Number ($U/fL$) remains small. The first attempt along these lines was carried out with a model incorporating a linearized balance equation which utilized the geopotential height only [9]. The results from this study were quite encouraging and they led to the present research. In this paper the complete, nonlinear form of the balance model was employed to obtain the three dimensional structure of the velocity field. Some sampling of the variability of the model was undertaken in the following manner. The complete nonlinear balanced stream function, which was computed from the geopotential, was compared to a nondivergent wind as derived from the observed velocities. Also several variations of the vertical motion (omega) equation were calculated in order to see the effect of input variation, surface friction, and latent heat in the model product.

After the final version of the model was completed, an attempt at verification of the calculated results was carried out. A comparison with the kinematic method of obtaining vertical motions proved to be of little use. However, another verification technique which consisted of subjectively correlating the derived vertical motion with the observed moisture distribution was more informative. The ultimate test of the diagnostic variables would be the prognostication from the derived initial state of the atmosphere. This experiment will be per-

---

[1] An abridged version of an M.A. thesis written at the University of California at Los Angeles.

[2] Past affiliation: University of California at Los Angeles.

formed in the near future by Krishnamurti, using a primitive model.

## 2. MODEL FRAMEWORK

The diagnostic numerical model that has been selected for this study is commonly called the nonlinear balanced model [8]. The equations pertaining to this system are presented below:

The balance equation,

$$f\nabla^2\psi+\beta\frac{\partial\psi}{\partial y}+2J\left(\frac{\partial\psi}{\partial x},\frac{\partial\psi}{\partial y}\right)=\nabla^2\varphi. \tag{1}$$

The omega equation,

$$\begin{aligned}\nabla^2\sigma\omega+f^2\frac{\partial^2\omega}{\partial p^2}=&f\frac{\partial}{\partial p}J(\psi,\nabla^2\psi+f)+\pi\nabla^2J(\psi,\theta)\\&-2\frac{\partial}{\partial p}\frac{\partial}{\partial t}\left[J\left(\frac{\partial\psi}{\partial x},\frac{\partial\psi}{\partial y}\right)\right]\\&-f\frac{\partial}{\partial p}(\nabla^2\psi\nabla^2\chi)+f\frac{\partial}{\partial p}\left(\omega\frac{\partial}{\partial p}\nabla^2\psi\right)\\&+f\frac{\partial}{\partial p}\left(\nabla\omega\cdot\frac{\partial}{\partial p}\nabla\psi\right)-f\frac{\partial}{\partial p}[\nabla\chi\cdot\nabla(\nabla^2\psi+f)]\\&-\nabla f\cdot\nabla\left(\frac{\partial}{\partial p}\frac{\partial\psi}{\partial t}\right)\\&-\pi\nabla^2(\nabla\chi\cdot\nabla\theta)+f\frac{\partial}{\partial p}(\mathbf{k}\cdot\nabla\times\mathbf{F})-\frac{R}{c_p p}\nabla^2H.\end{aligned} \tag{2}$$

The continuity equation,

$$\nabla^2\chi=-\frac{\partial\omega}{\partial p}. \tag{3}$$

The shear vorticity equation,

$$\begin{aligned}\nabla^2\frac{\partial}{\partial p}\frac{\partial\psi}{\partial t}=&-\frac{\partial}{\partial p}J(\psi,\nabla^2\psi+f)+\frac{\partial}{\partial p}[\nabla\chi\cdot\nabla(\nabla^2\psi+f)]\\&-\frac{\partial}{\partial p}\omega\frac{\partial}{\partial p}\nabla^2\psi+\frac{\partial}{\partial p}(\nabla^2\psi\nabla^2\chi)+f\frac{\partial}{\partial p}\nabla^2\chi\\&-\frac{\partial}{\partial p}\left(\nabla\omega\cdot\frac{\partial}{\partial p}\nabla\psi\right)-\frac{\partial}{\partial p}(\mathbf{k}\cdot\nabla\times\mathbf{F}).\end{aligned} \tag{4}$$

The symbols are defined as follows:

$c_p$ coefficient of specific heat at constant pressure
$f$ Coriolis parameter
$g$ acceleration of gravity
$\mathbf{k}$ unit vector in the $z$-direction
$p$ atmospheric pressure
$R$ specific gas constant
$\sigma$ static stability, $-(\alpha/\theta)\partial\theta/\partial p$
$T$ temperature
$\alpha$ specific volume
$\beta$ northward variation of Coriolis parameter
$\theta$ potential temperature
$\varphi$ geopotential
$\chi$ velocity potential for the irrotational component of velocity
$\psi$ stream function for the nondivergent component of velocity
$\rho$ density
$\omega$ the individual change of pressure ($dp/dt$)
$\nabla$ isobaric gradient operator
$\nabla^2$ Laplacian operator
$J$ Jacobian operator
$\mathbf{F}$ frictional force
$H$ diabatic heating (p.u.t.)
$\pi$ $(R/p)(p/p_0)^{R/c_p}$.

This set of equations defines a closed system in ($\psi$, $\omega$, $\chi$, $\partial(\partial\psi/\partial t)/\partial p$). The method of solving the nonlinear balanced model may be divided into three basic parts: the derivation of the nondivergent part of the horizontal wind, the solution of the omega equation, and the combination of the above results to form the complete three dimensional field of motion.

Several different variations are possible within the framework of the model. The original data may be inserted into the model in three different ways, each being a complete specification of the initial state. If the geopotential heights are used, no other parameter is necessary except the moisture. The nondivergent wind (stream function), and the thickness may then be calculated directly. If the geopotential is ignored, the streamlines, isotachs, and temperature may be substituted. The stream function is derived from the observed vorticity and the static stability is calculated from the temperature. A third method of input would be the inversion of the balance equation to obtain the geopotential using the observed winds only. The static stability is then obtained from the calculated geopotential. However, this method was not attempted in this study. The stream function, thickness or temperature, and the static stability, together with a frictional effect, will yield the first guess of the vertical motion. The omega equation, used for the first approximation, does not contain the nonlinear terms on the right hand side of equation (2). The first guess of the vertical motion is then used to calculate these nonlinear terms. The latent heating term is included at this point, since it is nonlinear in nature. An iterative process is performed until the difference between successive approximations is considered small. The final approximation of the vertical motion, the divergent part of the wind, which is a product of omega, and the stream function, define the complete three dimensional structure of the atmosphere.

The model utilizes the $x$, $y$, $p$ coordinate system on the beta plane with five levels of input data at 1000, 800, 600, 400, and 200 mb. The distances $x$, $y$ are measured toward the east and north respectively. Several variables are linearly interpolated to the intermediate levels (900, 700, 500, 300 mb.) where the vertical motion is solved. The

horizontal grid distance employed was 2° lat. by 2° long. beginning at 108°W. and extending to 56°W. The lowest latitude was 6°N. and the highest 34°N. This region contains approximately 500 grid points. The grid mesh is small enough to resolve wavelengths of the order of 800 km.

The simple centered finite difference method was used to calculate the various differentials in the equations of the model. A conventional method of relaxation as described by Thompson [19] is used to obtain the solutions of the partial differential equations. The boundary conditions for the omega equation were zero at the top (100 mb.) and bottom (1000 mb.), including a zero condition at the northern and southern edges. The stream function, velocity potential, and thickness tendency equations need only a two dimensional relaxation, requiring a zero condition at the northern and southern boundaries. The east-west boundaries were eliminated by adding six extra lines of grid points to the existing mesh. The last line of real data was parabolically interpolated over the six extra grid points to fit the real data at the other edge of the mesh, providing a cyclical continuity. The entire model was programed and solved on the IBM 7094.

## 3. SELECTION OF DATA INPUT

### STREAM FUNCTION

There are two completely different approaches to the problem of obtaining the nondivergent component of the wind. The conventional method involves the use of a form of the balance equation (1), which is a simplification of the divergence equation. This equation has certain undesirable properties in that a solution is not always possible from a given geopotential field [17], especially in the Tropics. The problem may be overcome if some known quantity is substituted into the Jacobian term for the stream function ($\psi$). Since the observed wind was analyzed, together with the geopotential, it was decided to insert the observed velocity components in place of $\partial\psi/\partial x$ and $\partial\psi/\partial y$. This substitution is a good approximation if the observed wind in the Tropics is quasi-nondivergent. However, for this substitution to be valid, it should be pointed out that the analysis of the observed wind should contain only the large-scale features of the velocity field [2].

Since the balance equation uses the geopotential as input, it was necessary to obtain an analysis of this field. If the analyses of the geopotential height value are performed without the aid of the wind field in the Tropics the result is a chaotic map bearing no resemblance to the flow patterns. Because the primary objective of the use of a diagnostic model is to represent the flow in an accurate manner, the analysis of the geopotential was adjusted to fit the calculated geostrophic gradient from the observed velocity field. At first thought, this might be considered a poor approximation in the Tropics. However, after adjusting the analysis, the changes were of the order of 20 m. or less in the majority of the observations. The final geopotential analysis was subjectively smoothed to include only the synoptic-scale effects in the data.

The alternate method, used to calculate the stream function, is described by Hawkins and Rosenthal [6]. The curl of the Helmholtz equation is written in the following form,

$$\nabla^2\psi=\zeta_{OB} \tag{5}$$

where the relative vorticity ($\zeta_{OB}$) is computed directly from the observed wind field. The author prefers to call this method the kinematic stream function. The boundary values at the north and south edges are calculated from the divergence of the observed wind with the following equations:

$$\nabla^2\chi=\delta_{OB} \tag{6}$$

$$\frac{\partial\psi}{\partial s}=-v_N+\frac{\partial\chi}{\partial N} \tag{7}$$

where $s$ is directed parallel to the boundary and $N$ is directed normal to the boundary. Equations (6), (7) were solved by "version 2" method as proposed by Hawkins and Rosenthal [6].

The products from these two different methods are illustrated in figure 1. The most obvious difference between the two stream functions is seen in the speed of the flow. The kinematic stream function speed is larger by a factor of two in some areas. The higher wind speeds agree more closely with the observed speeds. The general shape of the stream function pattern is almost identical in the two cases, indicating good agreement with respect to the direction of the flow. At the lower levels (not shown) differences in the shape do appear; however both stream functions were still highly correlated with the observed wind direction.

To compare the different stream functions in a more sensitive way, each was submitted as the nondivergent wind into the omega equation of the balanced model. All other input variables were held constant. The thickness temperature was arbitrarily utilized as the thermal parameter and the vertical motion equation was adiabatic and frictionless. The solution of the omega equation is presented in figure 2.

The most surprising result from this comparison is the relatively small difference in the overall pattern of the vertical motion fields at 500 mb. It appears that the changes in speed between the two stream functions did not affect the calculation of vertical motion to any great extent. Upon examination of the other levels nearer the ground (not shown) the agreement between the omega patterns deteriorates somewhat. Perhaps this can be blamed on the direction deviation between the two methods at the lower elevations.

From the comparisons presented above, it can be deduced that the technique of computing the kinematic stream function is probably as good as the balance formu-

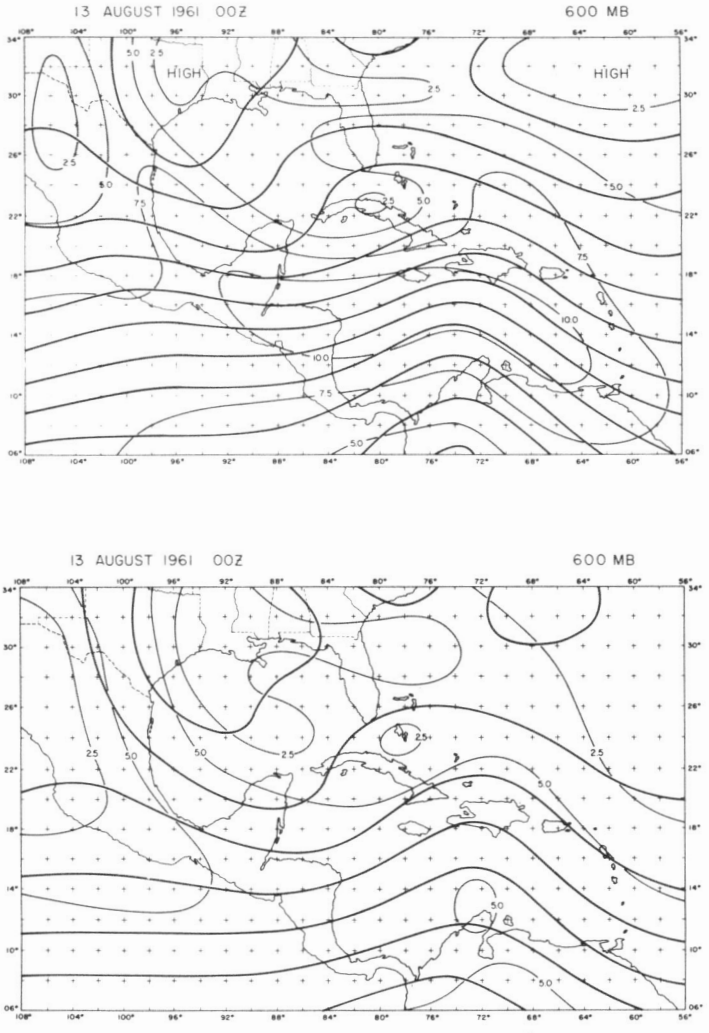


FIGURE 1.—Top: observed wind stream function. Bottom: balanced equation stream function. Heavy lines are stream function. Light, labeled lines are speeds given by the stream function in m./sec.

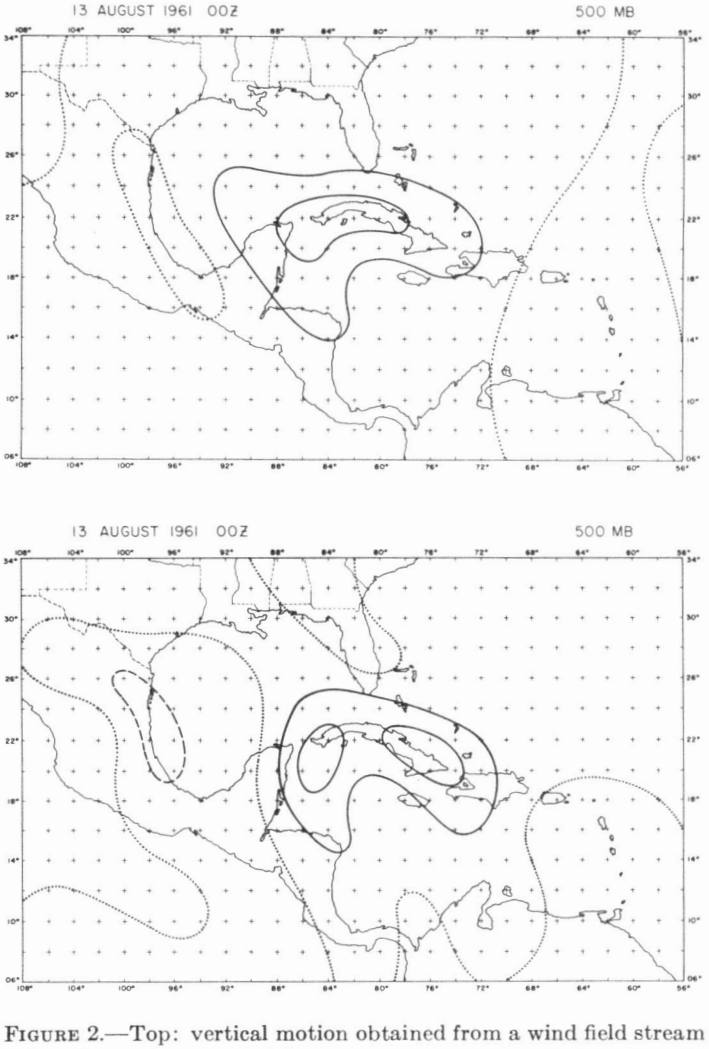


FIGURE 2.—Top: vertical motion obtained from a wind field stream function and geopotential thickness. Bottom: vertical motion obtained from a balance equation. Isolines are every $20\times10^{-5}$ mb./sec. (approximately 0.2 cm./sec.). Solid lines are sinking, dotted lines are neutral, and dashed lines are rising.

lation. Since the observed winds can be analyzed with more accuracy in the Tropics, implicit errors and approximations made in analyzing the geopotential field are eliminated by using the wind field stream function. Also, the error induced by satisfying the elliptic condition of the balance equation does not appear when the stream function is derived from the observed winds. Finally, it was shown that the kinematic stream function was a closer approximation of the true velocities. For these reasons, the wind field method of deriving the nondivergent wind was adopted throughout the rest of this paper.

## TEMPERATURE

The temperature distribution that is used in the numerical model may be obtained in several different ways. The most obvious method is to analyze, directly, the observed temperatures from the radiosonde data. The only computation necessary, before the analysis is performed, is a vertical average to eliminate any small-scale noise in the sounding. If the data network is dense enough, it becomes an easy task to analyze the synoptic-scale temperature patterns quite accurately from the observations even though the gradients are small in magnitude.

The alternate method of obtaining a temperature analysis is a thickness computation from the geopotential field. Since the geopotential is not a well-analyzed quantity in the Tropics, the temperature derived from such a field is subject to similar errors. In this particular research, the geopotential was adjusted to fit geostrophically the observed winds for the stream function calculation. Therefore, the thickness temperature implicitly contains the geostrophic approximation. This may not be in the best interest when an accurate temperature analysis is desired due to the relatively weak gradients of temperature being altered by the geostrophic adjustment.

The two types of temperature analysis are illustrated in figure 3. The observed temperature was linearly interpolated from the original input levels to the intermediate levels where the vertical motion is solved. The positions of the relative maximum and minimum are almost the

293-255 O - 68 - 4

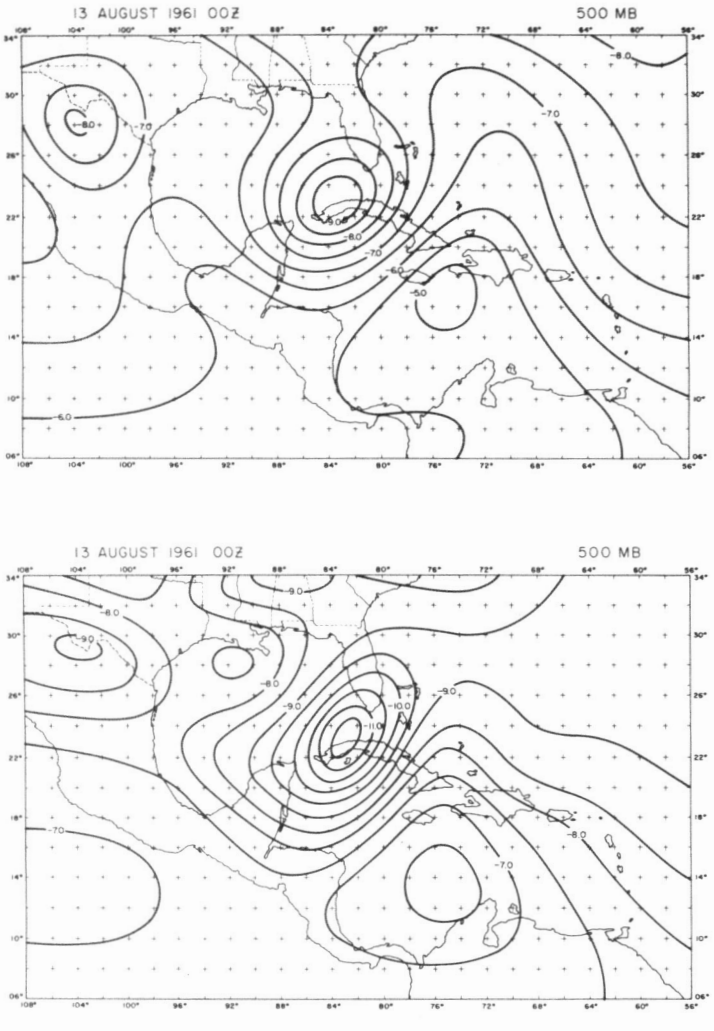


FIGURE 3.—Top: geopotential thickness temperature. Bottom: observed temperature. Isolines are drawn every 0.5°C.

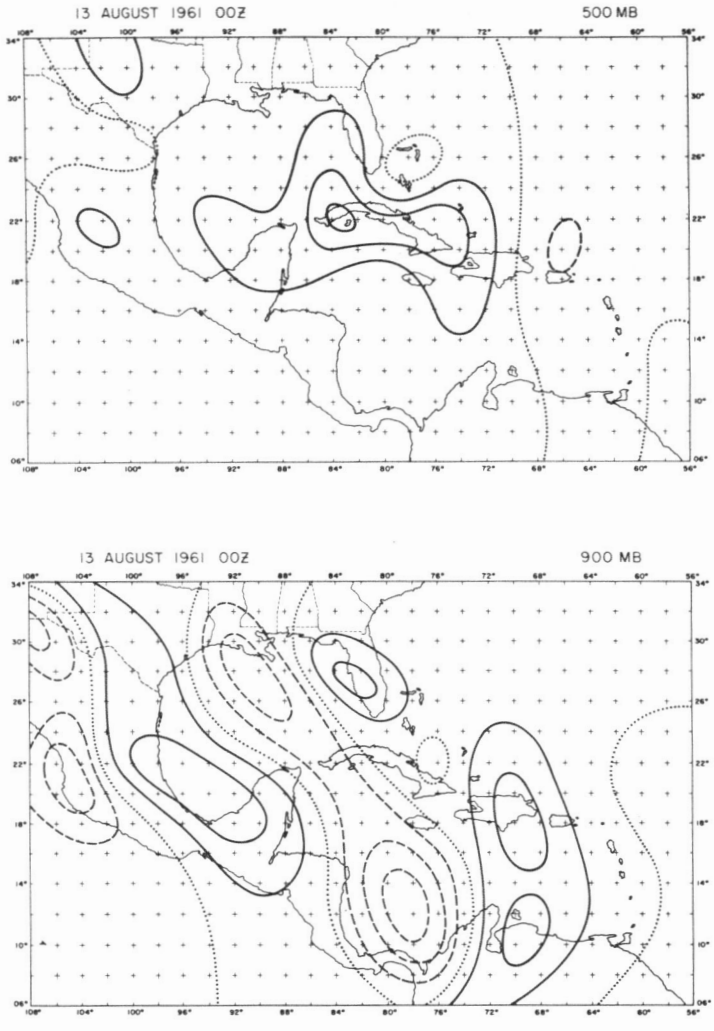


FIGURE 4.—Vertical motion obtained from observed temperature and wind field stream function. Isolines are every $20\times10^{-5}$ mb./sec. (approximately 0.2 cm./sec.). Solid lines are sinking, dotted lines are neutral, and dashed lines are rising.

same in the two temperature patterns. However, the observed temperature has more asymmetries in the analysis. The thickness gradients are somewhat weaker than the observed temperature at 500 mb., and the pattern agreement was much poorer at the lower levels. This may point to the low quality of the adjusted "geostrophic" geopotential near the ground. Since temperature appears in the omega equation as a gradient quantity, the magnitude of the temperature is not important, except for the static stability.

As in the case of the stream function comparison, the two variations of temperature input were submitted to the omega equation. The wind field stream function was used as the nondivergent wind in both cases. The model structure was kept exactly the same as described in the stream function comparison. The solution of omega using the observed temperature analysis is shown in figure 4. For a 500-mb. comparison the reader may refer to figure 2. The relative differences in temperature gradients between the two analyses becomes quite distinct in the omega patterns at 500 mb. The magnitude of the sinking air increased by 30 percent and a new center of rising motion appeared in the case of the inclusion of observed temperature. Also, the pattern of omega has changed considerably with the use of the different temperature analyses. The 900-mb. vertical motion shows well-organized systems when the observed wind and temperature are incorporated into the model.

From the evidence presented, it is not clear which type of temperature analysis is desirable in the evaluation of the balanced vertical motion. In the lower troposphere the observed temperature produced more organized patterns of omega than the thickness method. The observed temperature does have the advantage over the thickness with respect to the already discussed errors in the geopotential field. A definitive answer on which method is best cannot be drawn at this time. The observed temperature method will be included in all later experiments because of the relative ease of analysis.

## 4. EFFECT OF SURFACE FRICTION

The effect of the surface drag or frictional stress on the atmosphere may be included in the formulation of the balanced numerical model. Such an effect is usually some function of the surface wind speed and is included in the boundary conditions for the solution of the vertical motion [4]. The author chose instead to derive the frictional term as a forcing function (known quantity) in the omega equation. This enables the partitioning process as described by Krishnamurti, et al. [7] to separate the frictional part of the rising and sinking from the rest of the vertical motion.

The frictional term was obtained using the theory presented in Petterssen [13]. Using the empirical approximation of the stress, the final form of the forcing function term may be written:

$$+f\rho g C_D\left[\frac{\partial}{\partial x}\frac{\partial^2}{\partial p^2}(|\mathbf{V}|v)-\frac{\partial}{\partial y}\frac{\partial^2}{\partial p^2}(|\mathbf{V}|u)\right] \qquad (8)$$

where $|\mathbf{V}|$ is the wind speed, $u$ and $v$ are the components of the velocity, and the rest of the symbols are the same as in the model equation section. The drag coefficient ($C_D$) was held constant in the horizontal and its numerical value assumed to be $2.0\times10^{-3}$. Term (8) appears only in the 900-mb. omega equation with the rest of the levels having no frictional effects in their equations. Since the observed wind field was available at 1000 mb., a direct substitution was made into term (8). However, if the observed wind is not available, it is possible to write the $u$ and $v$ components in terms of the nondivergent and irrotational parts of the wind. Term (8) may then be evaluated internally in the model without the aid of the observed surface velocities.

The resulting omega distribution from this formulation is illustrated in figure 5. The partitioned frictional component is shown with the 1000-mb. wind vectors in order to point out the relations between the wind field and the frictional part of vertical motion. From this representation it is easily seen that the sinking motion corresponds with diffluent regions in the velocity field, and rising motion correlates well with confluent areas. The maximum intensity of the vertical motion field induced by the frictional term is approximately 0.5 cm./sec. From the partitioning it is shown that the frictional term is the same order of magnitude as the quasi-geostrophic terms in the omega equation. The absolute magnitude of the total vertical motion with friction at 900 mb., as shown in figure 5, increased considerably when compared with the frictionless omega in figure 4. The shape of the pattern remained more or less constant; however, almost every center has increased in intensity. The maximum rising motion is now nearly 1.0 cm./sec. in the vicinity of the closed circulation. It appears that friction is an important contributor in the generation of the vertical motion fields in the Tropics and should not be neglected in diagnostic studies.

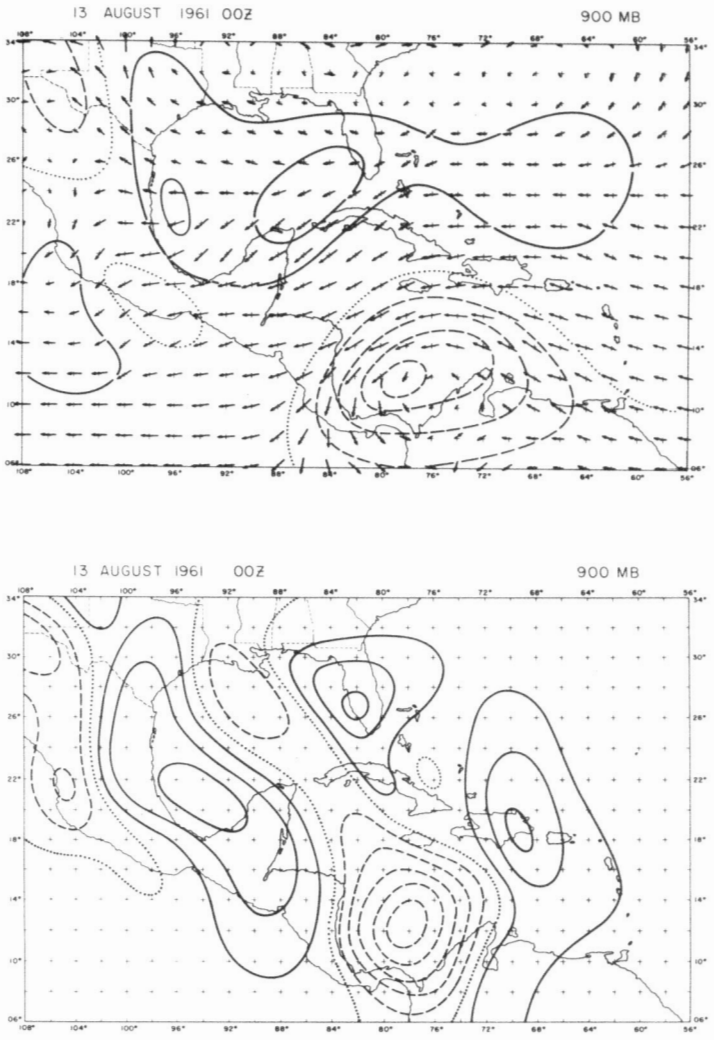


FIGURE 5.—Top: frictional component of the vertical motion with the 1000-mb. wind vectors. Solid lines are sinking, dotted lines are neutral, and dashed lines are rising. Isolines are drawn every $10\times10^{-5}$ mb./sec. Wind vectors are proportional to wind speed (10 m./sec.=0.4 cm.). Bottom: total vertical motion with friction added. Solid lines are sinking, dotted lines are neutral, and dashed lines are rising. Isolines are drawn every $20\times10^{-5}$ mb./sec.

## 5. ADDITION OF LATENT HEAT

According to some recent theoretical and numerical studies of Charney and Eliassen [3], Kuo [10], and others, the contribution of latent heat in the development of tropical storms appears to be of major importance. It was therefore reasoned that the inclusion of a latent heat effect in the diagnostic model should be attempted. In the middle latitudes, the addition of latent heat is relatively simple because it usually takes place in stable regions where the synoptic-scale motions are dominant. Several authors, Petterssen et al. [14] and Danard [5], have accomplished various types of latent heat inclusion with considerable success. However, this is not such an easy task in the Tropics, since the greatest amount of latent heat being produced is on a much smaller scale

than is considered in the numerical model [16]. Therefore a parameterization of the cumulus-scale latent heat is needed to incorporate this effect into the numerical model.

Both Charney and Eliassen [3] and Kuo [10] have derived a method by which the cumulus-scale latent heat contribution is estimated. Of the two methods, Kuo's formulation is the most complicated, involving actual calculations of the area covered by cumulonimbus towers. However, Charney and Eliassen's method was considered suitable for the needs of the diagnostic model. They use the three dimensional moisture flux of a column above the boundary layer as the parameter proportional to the amount of latent heat being released. In the case of the five level model, the convergence of moisture flux may be written:

$$I=\left[\frac{1}{g}\int_{900}^{0}\nabla\cdot\mathbf{V}pdq\right]-\frac{\omega_{900}\,q_{900}}{g} \tag{9}$$

where $q$ is the specific humidity. The first term is the horizontal moisture flux above the boundary layer and the second is the moisture leaving or entering the top of the boundary layer. In this particular model, 900 mb. was selected as the top of the boundary layer. The quantity ($I$) is calculated in the iterative process of the omega equation, since it is necessary to have the vertical motion at 900 mb. and the divergent wind with the stream function at the other levels. The specific humidity is taken directly from an analyzed mixing ratio at four levels. An example of the moisture convergence calculation is shown in figure 6. Each isoline of moisture convergence is equivalent to approximately 2.5°C. of warming a day if all the moisture coming into the column is precipitated.

The latent heat effect may be incorporated into the vertical motion equation at each level by forming the following heating term:

$$-\frac{RLg}{c_p p}\nabla^2\left[\frac{1}{q_s}\frac{1}{900}\frac{\partial q_s}{\partial p}AI\right] \tag{10}$$

where $A$ is an adjustment parameter of the moisture flux which will be referred to later, $L$ is latent heat of condensation, and $q_s$ is the saturation specific humidity. Before the heating term is activated in the omega equation at each grid point, it must pass three requirements. First, the moisture flux should be positive; obviously, clouds are not likely to form in a column where moisture divergence is taking place. Second, the synoptic-scale vertical motion at the level in question should be rising: this is analogous to the first requirement. And third, the relative humidity at the particular level must be greater than or equal to 60 percent. The latter prerequisite is imposed to eliminate the regions of dry air in which clouds are not forming. The grid points that satisfy these criteria are indicated with circles on the moisture convergence in figure 6.

The coefficient $A$ was adjusted to allow only a fraction of the moisture to be transformed into latent heat. This

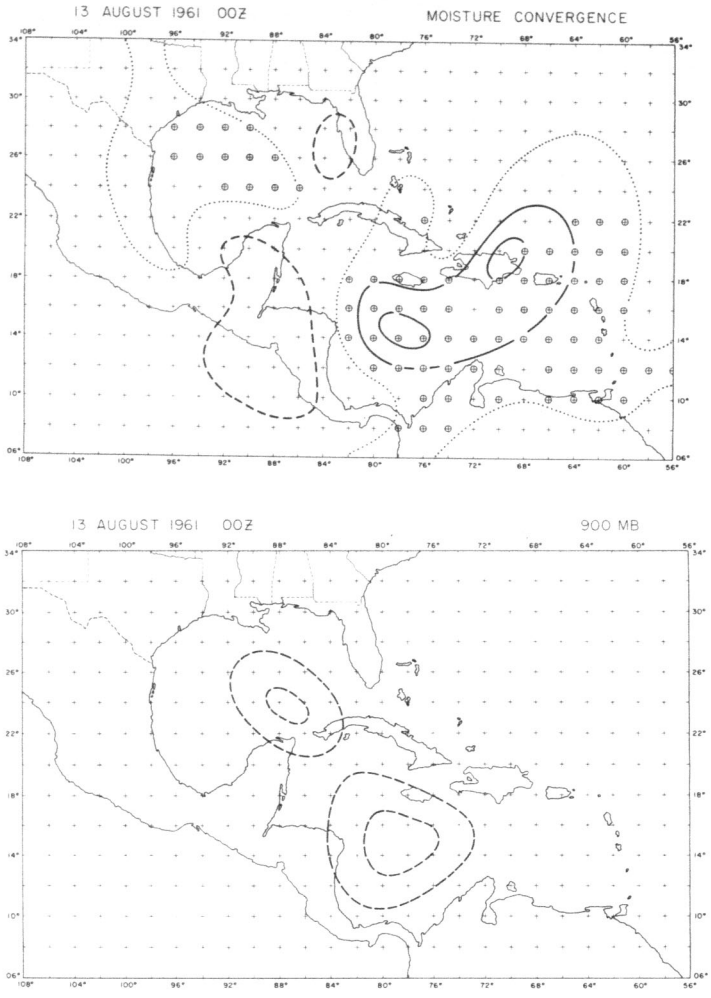


FIGURE 6.—Top: integrated three dimensional moisture flux. Solid lines are convergence, dotted lines are neutral, and dashed lines are divergence. Isolines are drawn every $100\times10^{-8}$ mb./m. Circled crosses are grid points of latent heat release. Bottom: latent heat component of the vertical motion. Dashed lines are rising motion drawn every $20\times10^{-5}$ mb./sec.

is, in fact, consistent with Kuo's findings, where he lets a portion of the moisture in his model raise the humidity and form the cloudiness in the column being considered. According to Kuo's theory, only about one-fourth of the moisture converging into the column actually falls out as rain. Several experiments were run in order to determine a suitable value for the coefficient as well as varying the three restrictions mentioned previously. The value finally chosen for the coefficient of the moisture flux was 0.2, which agrees with Kuo's work.

The latent heating component of the final solution of the omega equation is also illustrated in figure 6. Even when one-fifth of the moisture convergence is used in the diabatic term, the rising motion produced is still of the order of 0.5 cm./sec. The magnitude of this term places it alongside the quasi-geostrophic and frictional terms in importance. Upon careful examination of the drawing it is evident that some vertical motion is being

produced in regions of moisture divergence. This effect is due to the forcing function being specified at only a few, select grid points. Over the rest of the grid, the heating term is zero, allowing the relaxation technique to solve the differential equation by extrapolating to the zero condition at the boundaries. No method has yet been found to correct the existing problem. Barring this disturbing result, the solutions are very encouraging and reveal the importance of the contribution to the total vertical motion by latent heat parameterization.

## 6. COMPARISON OF BALANCED VS. KINEMATIC VERTICAL MOTION

The final version of the vertical motion, which includes latent heat and friction, is illustrated in figure 7. The magnitude of the rising center has now reached a maximum of 1.5 cm./sec. The average value of the synoptic-scale vertical velocity in the Tropics, as found by the balanced model numerical techniques, is approximately 0.5–1.0 cm./sec. Contrasting the vertical motion at 500 mb. (not shown) with 900 mb., the usual parabolic profile of omega is not found. Instead, many levels of nondivergence are present, giving a much more complicated structure to the vertical motion distribution in the Tropics.

A contrast between the numerical results and a kinematic vertical motion calculation was undertaken in order to show the difference in the two methods. The same observed wind fields used in the derivation of the stream function were employed in the kinematic omega calculation. The continuity equation was integrated with the observed divergence fields and a zero boundary condition at the surface. The results are shown in figure 7. It may be noted that the isolines of vertical velocity are $100\times10^{-5}$ mb./sec. for the kinematic vertical motion.

The contrast between the results of the two methods is quite remarkable. The kinematic omegas bear little or no resemblance to the numerical product although they are both derived from the same initial data. Reasons for the poor correlation between the different methods seem to be obscure. However, the lack of a sufficient number of observations to describe adequately the divergence field to sufficient accuracy is probably the largest reason for the poor kinematic result. The smooth omega patterns obtained by the balance model are derived from a well-defined stream function, whereas the kinematic vertical motion is derived directly from the observed divergence. Even though the nondivergent wind is computed from the observed velocity it is not nearly as sensitive to data inaccuracies as the divergence.

The results from this comparison are less than satisfying, since it is still not known how accurate and reliable the numerical method can be. It appears that some other method of verifying the numerical product must be attempted.

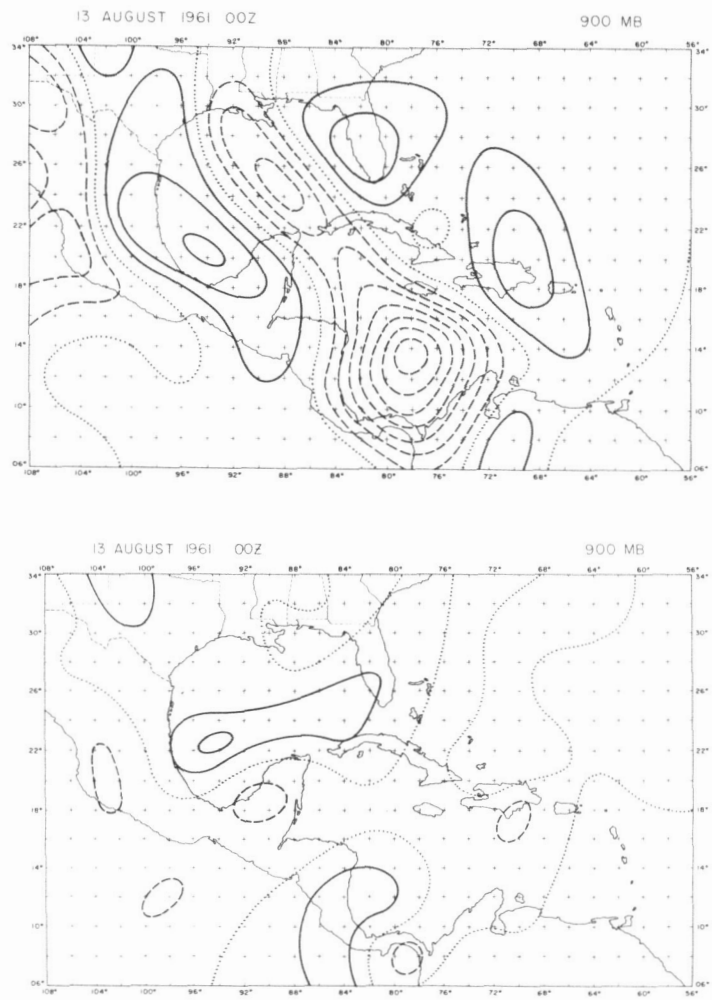


FIGURE 7.—Top: final vertical motion with friction and diabatic heating. Isolines are drawn every $20\times10^{-5}$ mb./sec. Solid lines are sinking, dotted lines are neutral, and dashed lines are rising. Bottom: kinematic vertical motion. Isolines are drawn every $100\times10^{-5}$ mb./sec. (approximately 1 cm./sec.). Solid lines are sinking, dotted lines are neutral, and dashed lines are rising.

## 7. VERTICAL MOTION-MOISTURE CORRELATION

In order to subject the balanced vertical velocities to further testing, a case study over the Caribbean area was accomplished for the period August 12–14, 1961. During this time a typical summer moisture surge or "easterly wave" was moving from east to west, toward Mexico. It should be pointed out that the wave did not develop into a tropical storm; however it did amplify during the latter part of the period.

The results of the balanced model for each 12-hr. segment were examined at great length and will appear in a later paper. The purpose here is to describe a possible moisture correlation with the balanced vertical motion. This is best illustrated in the form of cross sections (figs. 8, 9, 10). The top cross section is a vector representation of the rising and sinking air in partitioned form [7] at the four calculated levels. The bold arrowhead vector is the

total vertical velocity pointed in the direction of air flow. The lines to the immediate right of the vector are the various components of the omega equation with their direction indicating sinking or rising. The components are given below mathematically and descriptively in the order that they appear from left to right at each grid point.

| | |
|---|---|
| $f\frac{\partial}{\partial p}J(\psi, \nabla^2\psi+f)$ | differential vorticity advection |
| $\pi\nabla^2 J(\psi, \theta)$ | Laplacian of thermal advection |
| $-2\frac{\partial}{\partial p}\frac{\partial}{\partial t}\left[J\left(\frac{\partial\psi}{\partial x}, \frac{\partial\psi}{\partial y}\right)\right]$ | differential, time dependent deformation of the stream function |
| $-f\frac{\partial}{\partial p}(\nabla^2\psi\nabla^2\chi)$ | differential divergence-vorticity effect |
| $+f\frac{\partial}{\partial p}(\mathbf{k}\cdot\nabla\times\mathbf{F})$ | frictional effect |
| $-\frac{R}{c_p p}\nabla^2 H$ | diabatic heating. |

Actually there are 11 terms in the omega equation including friction and heating; however, the magnitudes of five terms were too small to be represented. The bottom cross section is a schematic representation of the cloud and moisture distribution. The information for this depiction was obtained from eight soundings along or near the 20° lat. line. The cloud distribution is derived from the surface weather reports and not satellite pictures.

The first pair of cross sections for August 12, 1961, exhibitsa high correlation between the moisture distribution and the proper sense of the vertical motion. The easterly wave or moisture surge is just entering the area of interest on the right. There is relatively strong sinking ahead of the wave which agrees well with the general desiccation of the air. The increase in moisture behind the wave can be associated with rising motion of the order of 0.5 cm. sec.$^{-1}$ From the partitioning, it can be deduced that the thermal advection term accounts for approximately 70 percent of the rising and sinking in the lower troposphere near the wave. The effects of diabatic heating in the rising air contribute only 20 percent during this map time.

In the next 24 hr. the moisture surge has moved nearly 20° of long. (fig. 9). The corresponding dipole, sinking and rising, of vertical velocities has moved as well, revealing an excellent correlation between the omegas and moisture. The rising air is strongest on the leading edge of the moisture surge with a new area of sinking air developing behind the easterly wave. Upon examination of the diabatic heating term it appears that latent heat is being released in an area of damped convective activity. This may be due to the course formulation used for the parameterization, and also the time of the observation. The magnitude of the heating term is almost 90 percent of the total vertical motion at some grid points.

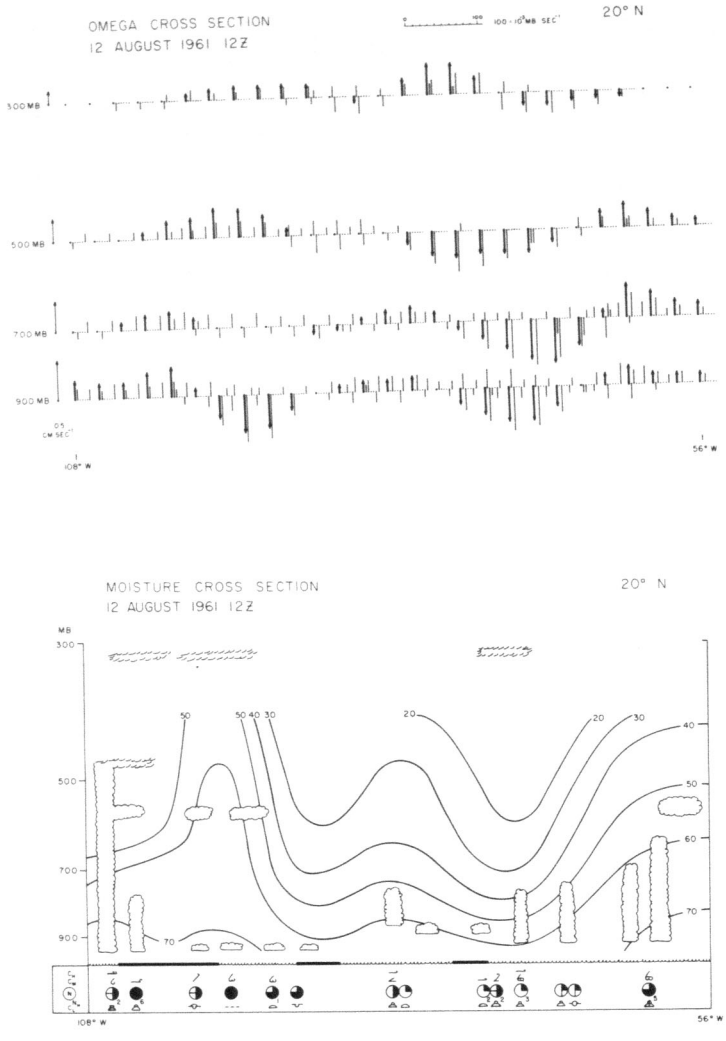


FIGURE 8.—Top: partitioned vertical motion. Heavy vector is the total, light lines are the components. Order at each grid point from left to right: total, vorticity, thermal, deformation, divergence, friction, and latent heat. Bottom: moisture and cloudiness. Solid lines are relative humidity every 10 percent. Clouds represented in schematic form.

At the final map time, August 14, 1961, the agreement between the moisture distribution and the vertical motion has deteriorated somewhat. However, the correlation at 900 mb., in particular, is still quite good. The entire moisture surge has continued to move toward the west with the corresponding movement of the trough (fig. 10). The drier air ahead of the wave has become more moist, possibly due to the change in sign of the vertical motion in the region. The correlation between the area of disturbed weather and the intense rising motion is encouraging even though the latent heat parameterization is somewhat simplified.

## 8. CONCLUDING REMARKS

From this research, it appears that the synoptic-scale vertical motions, as derived from the balance model, are about 1.0 cm./sec. in magnitude in large weather

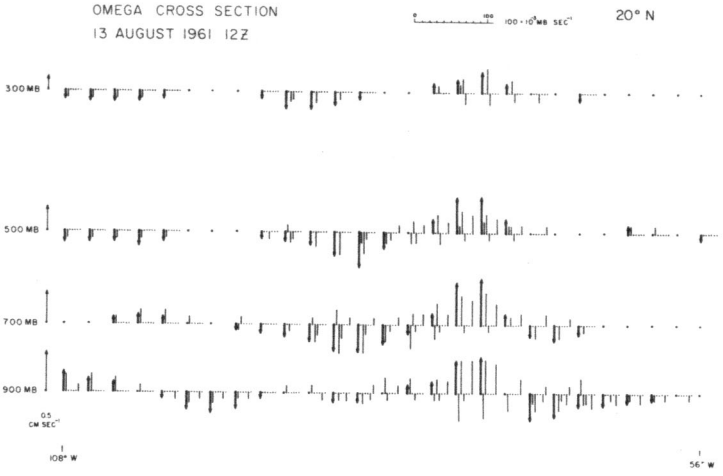


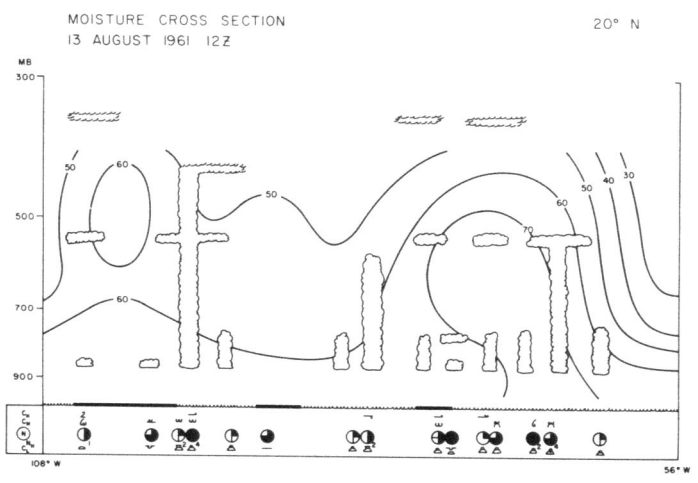


FIGURE 9.—Top: partitioned vertical motion. Heavy vector is the total, light lines are the components. Order at each grid point from left to right: total, vorticity, thermal, deformation, divergence, friction, and latent heat. Bottom: moisture and cloudiness. Solid lines are relative humidity every 10 percent. Clouds represented schematically.

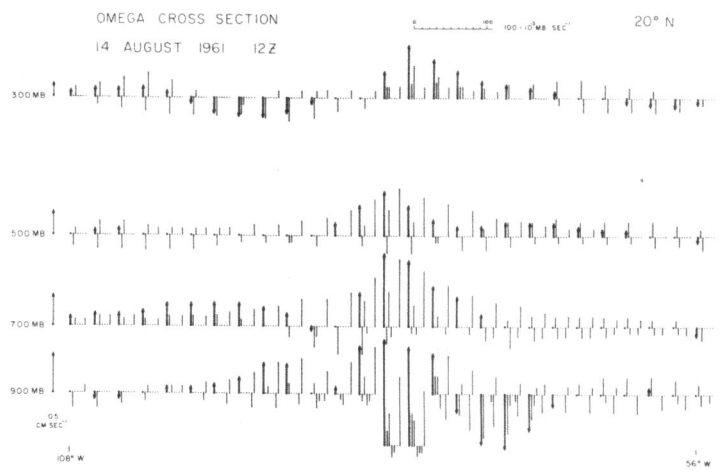


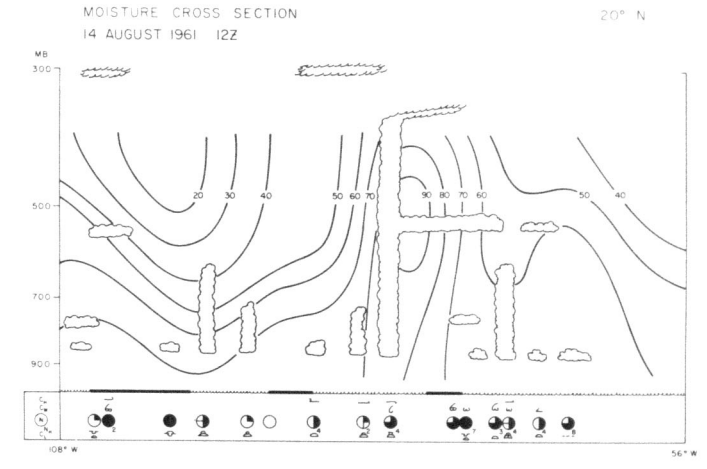


FIGURE 10.—Top: partitioned vertical motion. Heavy vector is the total, light lines are the components. Order at each grid point from left to right: total, vorticity, thermal, deformation, divergence, friction, and latent heat. Bottom: moisture and cloudiness. Solid lines are relative humidity every 10 percent. Clouds represented schematically.

disturbances. The most obvious objection to these results is the fact that the derived vertical motions are too small to have any effect on the moisture distribution. This may be a valid argument outside the influence of any large-scale circulation in the Tropics. The mesoscale and microscale weather systems overwhelm any effects produced by the weak rising or sinking. However, in a large disturbance, such as a traveling perturbation in the easterlies, the air remains under the influence of the wave for a considerable length of time.

During the case study just presented, a large mass of air behind the easterly wave was lifted approximately 50 mb. in 24 hr. If this were to take place over a longer time period, the synoptic-scale vertical motion has the capability of saturating air of 60 percent relative humidity. Since most of the weather in the Tropics is convective in nature, the dynamical rising and sinking merely increases the probability of thunderstorms by raising the relative humidity of the air. It is the author's contention that the synoptic-scale vertical motion in the Tropics can and does influence the convective activity to a large extent by the method previously noted.

The application of a numerical diagnostic model to the Tropics has given the meteorologist a useful tool in understanding the mechanism and processes of tropical weather systems. The appropriate choice of a stream function and temperature analysis along with the initial data preparation influence the product of the model to some extent. The inclusion of latent heat and friction altered the vertical motion fields considerably, proving that these effects are very important in the Tropics. The magnitudes of these terms were frequently 50 percent of the total omega.

The formulation of the complete nonlinear balanced model was quite adequate for use in the Tropics. It became obvious, when the partitioning was performed,

that certain terms in the omega equation were very small and could be neglected in future work. When the model was applied to a particular case study, a fairly good correlation was discovered between the calculated vertical motion and the observed moisture distribution. This fact gives insight into the reliability of the modeling results as well as the effects of the synoptic-scale vertical motion on the tropical weather.

The answers to a great number of questions may be revealed by a systematic dissection of all the major types of weather disturbances in the Tropics, using the numerical approach. The problem of prediction with numerical techniques can also be advanced by submitting as the initial state the results of an accurate diagnostic model.

## ACKNOWLEDGMENTS

This research could not have been undertaken without the guidance of Dr. Krishnamurti, who provided the author with the theoretical support, original computer programs, and many useful discussions. The help of Jan Paegle, who helped code many complicated machine programs, and the accurate plotting and tabulating of Steve Esbensen and Mirek Borowski is acknowledged. This work was performed with computer time donated by the Computing Facility at UCLA. Financial support was provided by AFCRL (Contract No. AF 19(628)-9777) and ESSA (Contract No. Cwb 11210).

## REFERENCES

1. J. G. Charney, "Integration of the Primitive and Balance Equations," *Proceedings of the International Symposium on Numerical Weather Prediction*, Meteorological Society of Japan, Tokyo, 1962, pp. 607–609.
2. J. G. Charney," A Note on Large-Scale Motions in the Tropics," *Journal of Atmospheric Science*, vol. 20, No. 6, Nov. 1963, pp. 607–609.
3. J. G. Charney and A. Eliassen,"On the Growth of the Hurricane Depression," *Journal of Atmospheric Science*, vol. 21, No. 1, Jan. 1964, pp. 68–75.
4. G. P. Cressman, "A Three-Level Model Suitable for Daily Numerical Forecasting," *Technical Memorandum* No. 22, National Meteorological Center, U.S. Weather Bureau, Washington, D.C., 1963, 32 pp.
5. M. B. Danard, "On the Influence of Released Latent Heat on Cyclone Development," *Journal of Applied Meteorology*, vol. 3, No. 1, Feb. 1964, pp. 27–37.
6. H. F. Hawkins and S. L. Rosenthal, "On the Computation of Stream Functions From the Wind Field," *Monthly Weather Review*, vol. 93, No. 4, Apr. 1965, pp. 245–252.
7. T. N. Krishnamurti, "A Study of a Developing Wave Cyclone," *Monthly Weather Review*, vol. 96, No. 4, Apr. 1968, pp. 208–217.
8. T. N. Krishnamurti, "A Diagnostic Balance Model for Studies of Weather Systems of Low and High Latitudes, Rossby Number less than 1," *Monthly Weather Review*, vol. 96, No. 4, Apr. 1968, pp. 197–207.
9. T. N. Krishnamurti and D. P. Baumhefner, "Structure of a Tropical Disturbance Based on Solutions of a Multi-Level Baroclinic Model," *Journal of Applied Meteorology*, vol. 5, No. 4, Aug. 1966, pp. 396–406.
10. H. L. Kuo, "On the Formation and Intensification of Tropical Cyclones Through Latent Heat Release by Cumulus Convection," *Journal of Atmospheric Sciences*, vol. 22, No. 1, Jan. 1965, pp. 40–63.
11. K. Miyakoda, "Some Characteristic Features of Winter-Time Circulations in the Troposphere and Lower Stratosphere," *Technical Report* No. 14, Department of Geophysical Sciences, University of Chicago, 1963, 84 pp.
12. C. E. Palmer, "Review of Tropical Meteorology," *Quarterly Journal of the Royal Meteorological Society*, vol. 78, No. 336, Apr. 1962, pp. 126–160.
13. S. Petterssen, *Weather Analysis and Forecasting* (2d Edition), The McGraw-Hill Book Co., Inc., New York, vol. 1, 1956, 428 pp. (see pp. 292–299).
14. S. Petterssen, D. L. Bradbury, and K. Pedersen, "Heat Exchange and Cyclone Development on the North Atlantic Ocean," *Technical Report*, Grant No. AF 19(604)-7230, University of Chicago, 1961, 76 pp.
15. H. Riehl, "Waves in the Easterlies and the Polar Front in the Tropics," *Miscellaneous Report* No. 17, Department of Meteorology, University of Chicago, 1945, 79 pp.
16. H. Riehl and J. S. Malkus, "On the Heat Balance in the Equatorial Trough Zone," *Geophysica*, Helsinki, vol. 6, No. 3/4, 1958, pp. 503–538.
17. F. G. Shuman, "Numerical Methods in Weather Prediction—The Balance Equation," *Monthly Weather Review*, vol. 85, No. 10, Oct. 1957, pp. 329–332.
18. D. Stuart, "Vertical Motion and the Baroclinic Mechanism of Rapid Upper-Level Cyclogenesis," *Final Report, California Rainfall Project*, Department of Meteorology, University of California at Los Angeles, 1961, 228 pp.
19. P. D. Thompson, *Numerical Weather Analysis and Prediction*, The MacMillan Co., New York, 1961, 170 pp.

[*Received June 30, 1967; revised October 23, 1967*]